



ISSN (Print) : 2320 – 3765  
ISSN (Online): 2278 – 8875

## International Journal of Advanced Research in Electrical, Electronics and Instrumentation Engineering

(An ISO 3297: 2007 Certified Organization)

Website: [www.ijareeie.com](http://www.ijareeie.com)

Vol. 6, Issue 4, April 2017

# Texture Analysis of Thyroid Ultrasound Images for Diagnosis of Cancerous Nodule Using ART1 Neural Network

Shrikant D. Kale<sup>1</sup>, Akash R. Dudhe<sup>2</sup>

Assistant Professor, Department Electronics & Telecommunication Engineering, Jagadambha College of Engineering  
& Technology, Arni Road, Yavatmal, Maharashtra, India<sup>1,2</sup>

**ABSTRACT:** A thyroid is largest endocrine gland, butterfly shape with two lobes which produces hormones that control metabolism body functions. The nodules are found in thyroid may be benign or malignant. The ultrasound (US) preferred over the other medical imaging modalities which is used to observe the subcutaneous body structures & internal organs for possible pathology or lesions. The physicians are deducing useful information concerning the tissue characterization and structure which is still subjective matter, Thus quantitative analysis of US images give the objective method for thyroid nodule diagnosis. In this paper, gray level co-occurrence matrix (GLCM) texture characterization techniques are used for feature extraction & extracted features are classified using adaptive resonance theory neural network (ART1) for diagnosis of thyroid nodule are described. The experimental results show the performance measure of classifier in terms of accuracy for the different vigilance parameter of ART1 neural network.

**KEYWORDS:** Thyroid nodule, ultrasound (US), GLCM, ART1 Classifier.

### I.INTRODUCTION

A thyroid is largest endocrine gland in the body, a butterfly shaped organ compose of the cone like lobes. It is located in the lower part of the neck below the Adam apple. The thyroid gland produces the T3 & T4 hormones that affects the heart rate, cholesterol level, body weight, energy level, mental state and controls a host of other body functions. Thus the function of thyroid is to regulate the body metabolism<sup>[1]</sup>. The thyroid diseases are common worldwide. In India too, there is significant burden of thyroid diseases. According to a projection from various studies on thyroid disease, it has been estimated that about 42 million people in India suffer from thyroid diseases. It covers the main five thyroid gland disease included the main five thyroid diseases: Hypothyroidism, Hyperthyroidism, Goiter, Autoimmune Thyroiditis, Thyroid cancer<sup>[2]</sup>.

A National Cancer Registry program (NCRP) maintains the reliable data of cancer patient on the magnitude & pattern of cancer in India. The projection of thyroid cancer cases in year of 2010 is around 16,215 & by the year of 2020 goes up to 19,113. The cases of malignant thyroid nodule are found to be more in female to that of male. The projection of thyroid cancer in female for year of 2010, 2015 & 2020 is 11,751; 12,808 & 13,955 significant over male i.e. 4,464; 4,798 & 5,158 for the respective years. The other figures of thyroid disease are turn out to be significant in the Indian context. The preferred diagnosis method used for possible lesions are ultrasonography.<sup>[2]</sup>

All radiological modalities like ultrasound, CT, Scintigraphy, SPECT, MR, PET, X-rays etc. play an important role in process of disease diagnosing and have become major evidence to ensure disease. But ultrasound (US) possesses a rare combination of advantages including portability, invasive, real-time data acquisition and affordability<sup>[3]</sup>. US are a diagnostic imaging tool used to visualize subcutaneous body structures and internal organs for possible pathology or lesions. The physicians are deducing useful information concerning the tissue characterization and structure. Thus, US have become an invaluable tool for the accurate diagnosis and follows up of different pathologies in a variety of tissues and organs<sup>[4]</sup>.



# International Journal of Advanced Research in Electrical, Electronics and Instrumentation Engineering

(An ISO 3297: 2007 Certified Organization)

Website: [www.ijareeie.com](http://www.ijareeie.com)

Vol. 6, Issue 4, April 2017

The detection of the pathological diseases such as thyroid nodule by physicians is still subjective matter & while making manual diagnosis from images, some relevant information need not to be recognized by human visual system. In the suspicious cases FNA, Cytological test are done to find the malignancy risk. Thus to provide the objectification for disease diagnosis the various texture characterization techniques are utilized which draws statistical information from US image. Thus quantitative information is used to classify into benign & malignant thyroid nodule.

## II. RELATED WORK

There have been various attempts towards the subjective techniques for diagnosis of thyroid gland nodule. Some of the earlier research was the 13 GLCM texture & geometric features extracted from thyroid images by region based active contour segmentation method & classified using SVM, KNN and Bayesian <sup>[1]</sup>.

In <sup>[2]</sup>, the Contourlet Transform (CT) using LP and DFB filters to the 3rd level decomposition are used for detection hypoechoic and isoechoic nodules from normal thyroid nodule. A Gaussian kernel SVM classifier is applied along the SFFS algorithm with or without coefficient thresholding. In <sup>[16]</sup>, the texture features based on the CT using different types of filters banks with a selection scheme SFFS algorithm were classified by k-NN algorithm.

In [6], a novel computational approach using Radon Transform for the thyroid tissue characterization of US image were utilized. Supervised classification experimentation using KNN(k=5), SVM with polynomial kernel was done to differentiate normal and nodular thyroid US images for detection malignancy risk. In <sup>[7]</sup>, the normal and hypoechoic nodule were classified using 2 First-order and 168 co-occurrence features drawn from manual rectangular ROI & PCA for optimal subset using Binary Logistic Regression.

In <sup>[8]</sup>, a novel approach that correlates thyroid malignancy, LBP, FLBP, and FLGH Ultrasound texture features which discriminated by SVM with linear, polynomial and Gaussian kernel with or without fusion of texture using 10 fold cross validation or 1 way ANOVA. In <sup>[9]</sup>, a novel fuzzy feature extraction method (FLBP). The FLBP approach was experimentally evaluated using supervised SVM with linear, polynomial, radial basis, sigmoid kernel for classification of nodular and normal thyroid US images. In <sup>[10]</sup>, the joint texture analysis on US and Cytological images were processed to optimally highlight the cancerous region in same image. The 20 textural features were generated which contain 4 GH, 10 GLCM and 6 RLM from US image. 20 morphological and textural features were extracted from segmented nuclei of Cytological image. An SVM classifier with 2nd degree polynomial kernel & Bayesian with quadratic kernel were used in distinguishing correctly low from high-risk thyroid nodules.

## III. MATERIAL & METHOD

Medical ultrasound images of thyroid gland are selected for texture analysis in experimental work. These ultrasound images contained some of abnormal images having benign thyroid nodule (non cancerous) and malignant thyroid nodule (cancerous). The total 85 thyroids US images were used which contains total 48 cancerous and 37 non-cancerous was selected in database. These thyroid images are available in image gallery of Wilmington Endocrinology PA on website. The image size of  $546 \times 410$ , with 24 bit depth size, true color image, format of images are JPEG.

The Matlab R2010a software is used for experimental work. The preprocessing steps required for the analysis is gray scale conversion & image resizing into  $256 \times 256$  of true color images selected in database. Then GLCM texture feature extraction & classification of texture feature are carried out & described in following section.

### A. TEXTURE ANALYSIS METHOD

The analysis of texture parameters is a useful way of increasing the information obtains from medical images. It is an ongoing field of research, with applications ranging from the segmentation of specific anatomical structures and the detection of lesions, to differentiation between pathological and healthy tissue in different organs. Texture analysis uses radiological images obtained in routine diagnostic practice, but involves an ensemble of mathematical computations performed with the data contained within the images <sup>[13]</sup>.



# International Journal of Advanced Research in Electrical, Electronics and Instrumentation Engineering

(An ISO 3297: 2007 Certified Organization)

Website: [www.ijareeie.com](http://www.ijareeie.com)

Vol. 6, Issue 4, April 2017

According to the methods employed to evaluate the inter-relationships of the pixels, the forms of texture analyses are categorized as structural, model-based, statistical and transform methods<sup>[11]</sup>.

## 1. STRUCTURAL METHODS

This represents texture by the use of well-defined primitives. In other words, a square object is represented in terms of the straight lines or primitives that form its border. The advantage of these methods is that they provide a good symbolic description of the image. On the other hand, it is better for the synthesis of an image than for its analysis.<sup>[13]</sup>

## 2. MODEL-BASED METHODS

Here an attempt is made to represent texture in an image using sophisticated mathematical models (such as fractal or stochastic). The model parameters are estimated and used for the image analysis. The disadvantage is the computational complexity involved in the estimation of these parameters<sup>[13]</sup>.

## 3. STATISTICAL APPROACHES

These are based on representations of texture using properties governing the distribution and relationships of grey-level values in the image & normally achieve higher discrimination indexes than the structural or transform methods<sup>[13]</sup>.

## 4. TRANSFORM METHODS

The texture properties of the image may be analyzed in a different space, such as the frequency or the scale space. These methods are based on the Radon, Gabor or Wavelet transform. The Wavelet transform is the most widely used because of the ease with which it may be adjusted to the problem in question<sup>[13]</sup>.

### ***B. TEXTURE FEATURE EXTRACTION METHODS***

Medical images possess a vast amount of texture information relevant to clinical practice. For example, US images of tissues are not capable of providing microscopic information that can be assessed visually. However, histological alterations present in some illnesses may bring about texture changes in the US image that are amenable to quantification through texture analysis. This has been successfully applied to the classification of pathological tissues from the liver, thyroid, breasts, kidneys, prostate, heart, brain and lungs<sup>[13]</sup>.

The most commonly used texture features are Gray Level Histogram, Run-length matrix, Gray Level Co-occurrence matrix, contour let transform, Wavelets transform, Radon Transform, Local Binary Pattern, Fuzzy Local Binary Pattern, Fuzzy local Gray Histogram.

These texture feature found in literature of texture analysis on ultrasound medical images of thyroid gland for detection of thyroid nodule as a benign or malignant tissue from normal one. In this paper, gray level co-occurrence matrix (GLCM) based texture feature extraction approach is followed which explain next in detail. The 22 texture features extracted from GLCM are described mathematically in table 1.

## 1. GRAY LEVEL CO-OCCURRENCE MATRIX

Using histograms in calculation will result in measures of texture that carry only information about distribution of intensities, but not about the relative position of pixels with respect to each other in that texture. Using a statistical approach such as co-occurrence matrix will help to provide valuable information about the relative position of the neighboring pixels in an image.

Given an gray scale image  $I$ , of size  $N \times N$ , the co-occurrence matrix  $P$  can be defined as



# International Journal of Advanced Research in Electrical, Electronics and Instrumentation Engineering

(An ISO 3297: 2007 Certified Organization)

Website: [www.ijareeie.com](http://www.ijareeie.com)

Vol. 6, Issue 4, April 2017

$$P(i, j) = \sum_{x=1}^N \sum_{y=1}^N \begin{cases} 1 & ; I(x, y) = i \text{ and } I(x + \Delta x, y + \Delta y) = j \\ 0 & ; \text{otherwise} \end{cases} \quad (1)$$

Here, the offset  $(\Delta x, \Delta y)$ , is specifying the distance between the pixel-of-interest and its neighbour. Note that the offset  $(\Delta x, \Delta y)$  parameterization makes the co-occurrence matrix sensitive to rotation. Choosing an offset vector, such that the rotation of the image is not equal to 180 degrees, will result in a different co-occurrence matrix for the same (rotated) image. This can be avoided by forming the co-occurrence matrix using a set of offsets sweeping through 180 degrees at the same distance parameter  $\Delta$  to achieve a degree of rotational invariance (i.e.,  $[0 \ \Delta]$  for 0 degree: P horizontal,  $[-\Delta, \ \Delta]$  for 45 degree: P right diagonal,  $[-\Delta \ 0]$  for 90 degree: P vertical, and  $[-\Delta \ -\Delta]$  for 135degree: P left diagonal).

The texture features extracted using GLCM matrix from the selected thyroid ultrasound images are given by equations as follows:

$$\text{Autocorrelation} \quad \sum_i \sum_j (i \cdot j) P(i, j) \quad (2)$$

$$\text{Contrast} \quad \sum_i \sum_j |i - j|^2 P(i, j) \quad (3)$$

$$\text{Correlation - I} \quad \sum_i \sum_j \frac{(i - \mu_x) \cdot (j - \mu_y) P(i, j)}{\sigma_x \cdot \sigma_y} \quad (4)$$

$$\text{Correlation - II} \quad \sum_i \sum_j \frac{(i \cdot j) P(i, j) - \mu_x \mu_y}{\sigma_x \cdot \sigma_y} \quad (5)$$

$$\text{Cluster Prominence} \quad \sum_i \sum_j (i + j - \mu_x - \mu_y)^4 P(i, j) \quad (6)$$

$$\text{Cluster Shade} \quad \sum_i \sum_j (i + j - \mu_x - \mu_y)^3 P(i, j) \quad (7)$$

$$\text{Dissimilarity} \quad \sum_i \sum_j |i - j| P(i, j) \quad (8)$$

$$\text{Energy} \quad \sum_i \sum_j |P(i, j)|^2 \quad (9)$$

$$\text{Entropy} \quad - \sum_i \sum_j P(i, j) \log(P(i, j)) \quad (10)$$

$$\text{Homogeneity- I} \quad \sum_i \sum_j \frac{P(i, j)}{1 + |i - j|} \quad (11)$$

$$\text{Homogeneity- II} \quad \sum_i \sum_j \frac{P(i, j)}{1 + |i - j|^2} \quad (12)$$

$$\text{Maximum Probability} \quad \max_{i, j} P(i, j) \quad (13)$$

Notation & expression used for calculating the GLCM statistics are as shown below.

Notation	Meaning	
L	Gray-level quantization	
N	Mean value of $p(i, j)$ .	
$P_x(i)$	$\sum_{j=1}^L P(i, j)$	(14)
$P_y(i)$	$\sum_{i=1}^L P(i, j)$	(15)
$\mu_x$	$\sum_i \sum_j i \cdot P(i, j)$	(16)
$\mu_y$	$\sum_i \sum_j j \cdot P(i, j)$	(17)
$\sigma_x^2$	$\sum_i \sum_j (i - \mu_x)^2 \cdot P(i, j)$	(18)
$\sigma_y^2$	$\sum_i \sum_j (j - \mu_y)^2 \cdot P(i, j)$	(19)

## C. CLASSIFICATION METHOD

For the experimental evaluation of texture feature extracted from ultrasound thyroid gland images using GLCM matrix method was classified by neural network adaptive resonance theory. The ART1 network used in experiment, in which binary features were given as the input to the F1(a) layer. The feature space vectors were converted in binary feature space by utilizing the mean of each feature vectors as shown in figure 1.

The adaptive resonance theory (ART1) is a class of self organizing neural architectures raised by S. Grossberg and A. Carpenter in 1976 that cluster the feature space & produce appropriate weight vector. An advantage using ART neural network is that remains open to new learning without washing away previously learned patterns i.e. plasticity. The ART neural network is stable one, which does not returns the pattern to previous cluster.

# International Journal of Advanced Research in Electrical, Electronics and Instrumentation Engineering

(An ISO 3297: 2007 Certified Organization)

Website: [www.ijareeie.com](http://www.ijareeie.com)

Vol. 6, Issue 4, April 2017

The unsupervised ARTs named as ART1, ART2 for binary & continuous feature vectors & are similar to many iterative clustering algorithms where the terms 'nearest' & 'closer' are modified by introducing the concept of 'resonance'. Resonance is just a matter of being within a certain threshold of a second similarity measure.

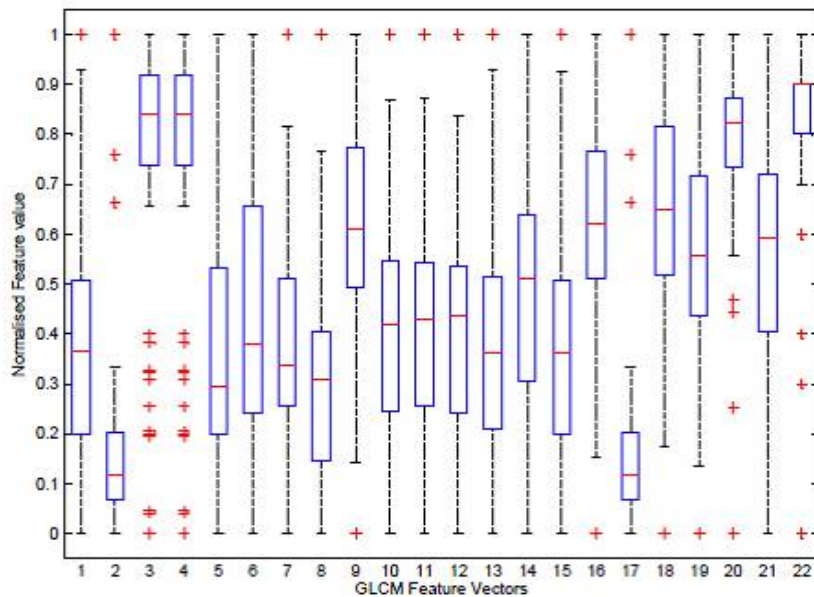


Fig. 1 Boxplot of GLCM Feature Vectors

The basic ART system is unsupervised learning model. It typically consists of 1) a comparison layer 2) a recognition layer composed of neurons, 3) a vigilance parameter & 4) a reset module. The ART1 neural network architecture is as shown in Fig. 2.

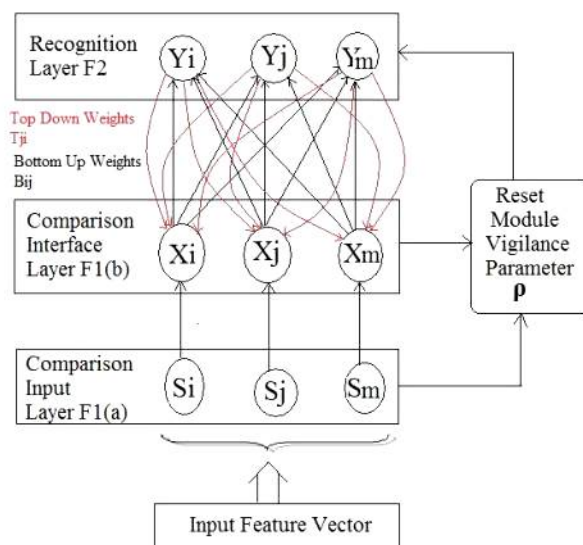


Fig. 2 ART1 Neuron Network Architecture



# International Journal of Advanced Research in Electrical, Electronics and Instrumentation Engineering

(An ISO 3297: 2007 Certified Organization)

Website: [www.ijareeie.com](http://www.ijareeie.com)

Vol. 6, Issue 4, April 2017

## 1. COMPARISON LAYER

The comparison layer takes an input vector & transfers it to its best match in the recognition layer. Its best match is the single neuron whose set of weights most closely matches the input vector.

## 2. RECOGNITION LAYER

Each recognition layer neuron outputs a negative signal proportional to that neurons quality to match to the input vector to each of the other recognition layer neurons & inhibits their output accordingly. In this way the recognition layer exhibits lateral inhibition, allowing each neuron in it to represent a category to which input vectors are classified.

## 3. VIGILANCE PARAMETER

After the input vector is classified, a reset module compares the strength of the recognition match to a vigilance parameter. The vigilance parameter has considerable influence on the system: Higher vigilance produces highly detailed memories, Lower vigilance results in more general memories.

## 4. RESET MODULE

The reset module compares the strength of the recognition match to the vigilance parameter. If the vigilance threshold is met, then training commences. Otherwise, if the match level does not meet then vigilance parameter, then the firing recognition layer neuron is inhibited until a new input vector is applied Training commences only upon completion of a search procedure. In the search procedure, the recognition neurons are disabled one by one by the reset function until the vigilance parameter is satisfied by a recognition match. If no committed recognition neurons match meets the vigilance threshold, then an uncommitted neuron is committed & adjusted towards matching the input vector.

The ART1 training algorithm is as follows

- Step 1: Initialize parameters,  $L > 1$  and  $0 < \rho \leq 1$ .  
Initialize weights:  $0 < b_{ij} < \frac{L}{L-1+n}$ ,  $t_{ji}(0) = 1$
- Step 2: While stopping condition is false, perform steps 3-14.
- Step 3: For each training input do steps 4-13.
- Step 4: Set activation of all F2 units to zero.  
Set activation of all F1(a) units to input vector  $s$ .
- Step 5: Compute norm of  $s$ :  $\|s\| = \sum_i S_i$
- Step 6: Send input signal from F1(a) to F1(b) layer:  $X_i = S_i$
- Step 7: For each F2 node that is not inhibited  
If  $y_J \neq -1$ , then  $y_j = \sum_i b_{ij} X_i$
- Step 8: While reset is true, perform steps 9-12.
- Step 9: Find  $J$  such that  $y_J \geq y_j$  for all nodes  $j$ .  
If  $y_j = -1$ , then all the nodes are inhibited and this pattern cannot be clustered.
- Step 10: Recompute activation  $x$  of F1(b):  $x_i = s_i t_{ji}$
- Step 11: Compute norm of vector  $x$ :  $\|x\| = \sum_i X_i$
- Step 12: Test for reset : If  $\frac{\|x\|}{\|s\|} < \rho$ , then  $y_J = -1$  (inhibit node  $J$ ) and continue executing steps 8 again  
If  $\frac{\|x\|}{\|s\|} \geq \rho$ , then proceed to the step 13.
- Step 13: Update the weights for node  $J$ :  
$$b_{iJ}(\text{new}) = \frac{L X_i}{L-1 + \|x\|}$$
$$t_{ji}(\text{new}) = x_i$$
- Step 14: Test for stopping condition.

# International Journal of Advanced Research in Electrical, Electronics and Instrumentation Engineering

(An ISO 3297: 2007 Certified Organization)

Website: [www.ijareeie.com](http://www.ijareeie.com)

Vol. 6, Issue 4, April 2017

## IV. EXPERIMENTAL RESULT

The GLCM calculation was done for the different value of the offset & up to 15 pixel distance for each offset. Then the above mentioned 22 texture features was extracted for the each offset & pixel distance from the US thyroid images. There are total 85 samples, each sample have 22 feature element which is applied to the input layer F1(a) & the output layer F2 have two cluster. The experimental evaluation of this feature vectors were done by ART1 neural network classifier. The ART1 neural network were simulated & performance measure of the network evaluated from the known ground truth in terms of TP (True Positive), FN (False Negative), TN (True Negative), FP (False Positive). Then the ACC (Accuracy), PPV (Positive Predictive Value), NPV (Negative Predictive Value), Sp (Specificity), Se (Sensitivity) & GM (G -Mean) were calculated. Fig.3. (a) & (b) shows the ROC & Confusion Matrix of ART1 Classifier with with offset [-4 0].

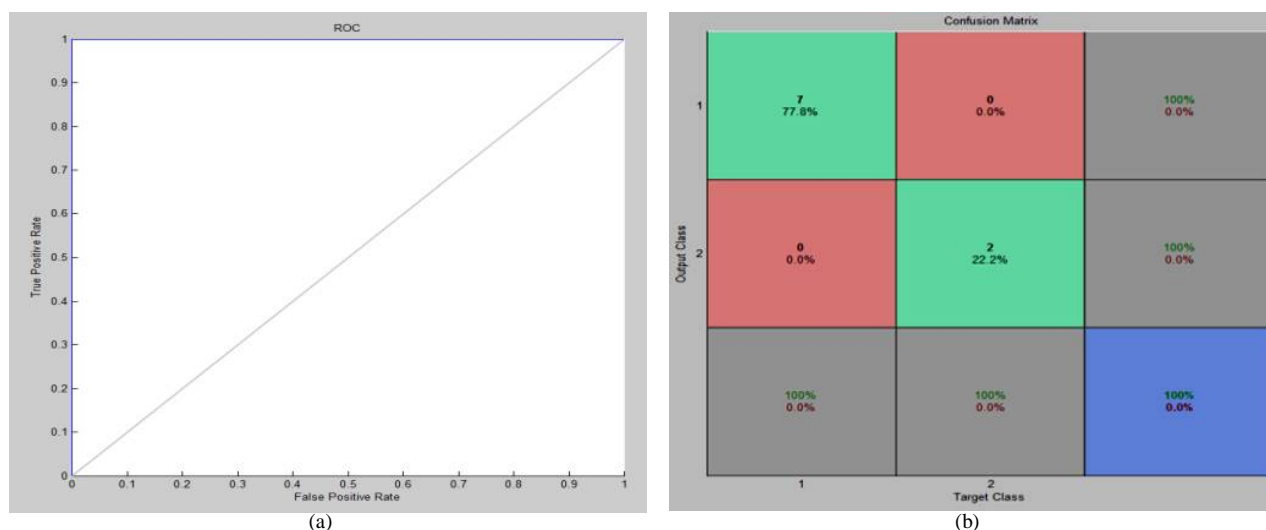


Fig. 3 (a) ROC of ART1 classifier & (b) Confusion Matrix of ART1 classifier with offset [-4 0]

GLCM Offset/Vigilance Parameter	Acc (%)	PPV (%)	NPV (%)	Sp (%)	Se (%)	GM
V <sub>4</sub> /0.6-0.9	100	100	100	100	100	1.414
V <sub>4</sub> /0.3	88.89	100	66.67	85.71	100	1.363
H <sub>6</sub> /0.1,0.4-0.9	88.89	75	100	100	83.33	1.354
LD <sub>5</sub> /0.2	88.89	80	100	100	80	1.342
RD <sub>1</sub> /0.7,0.8, LD <sub>15</sub> /0.9	88.89	100	83.33	75	100	1.323
V <sub>8</sub> /0.3	77.78	100	33.33	75	100	1.323
V <sub>4</sub> /0.1,0.2,0.4,0.5	77.78	100	50	71.43	100	1.309
V <sub>15</sub> /0.6, RD <sub>3</sub> /0.1-0.4,0.5, RD <sub>6</sub> /0.1,0.4, RD <sub>15</sub> /0.7	77.78	100	60	66.67	100	1.291
H <sub>11</sub> /0.1-0.8, LD <sub>5</sub> /0.1,0.3-0.8	77.78	66.67	100	100	60	1.265
V <sub>7</sub> /0.1,0.2, LD <sub>15</sub> /0.8	77.78	80	75	80	75	1.245
LD <sub>15</sub> /0.8	77.78	75	80	75	80	1.245
H <sub>13</sub> /0.2, V <sub>5</sub> /0.4-0.6,0.8,0.9, RD <sub>15</sub> /0.1-0.4,	77.78	66.67	83.33	66.67	83.33	1.255
V <sub>14</sub> /0.1,0.2, LD <sub>12</sub> /0.4	77.78	71.43	100	100	50	1.255
RD <sub>15</sub> /0.4, LD <sub>6</sub> /0.6,	77.78	83.33	66.67	83.33	66.67	1.255

Table 1: Simulation results of ART1 Neural Network



ISSN (Print) : 2320 – 3765  
ISSN (Online): 2278 – 8875

# International Journal of Advanced Research in Electrical, Electronics and Instrumentation Engineering

(An ISO 3297: 2007 Certified Organization)

Website: [www.ijareeie.com](http://www.ijareeie.com)

Vol. 6, Issue 4, April 2017

## REFERENCES

- [1] Eystratios G. Keramidas, Dimitris K. et al, "Efficient and effective ultrasound image analysis scheme for thyroid nodule detection", Lecture Notes Computer Science 4633:PP. 1052–1060, 2007.
- [2] Ambika G. Unnikrishnan, Usha V. Menon, "Thyroid disorders in india : A epidemiological perspective", Indian Journal of Endocrinology and Metabolism, vol. 15 , suppliment 2, PP. 78-81, 2011.
- [3] Ramnath Takiar, Deenu Nadayil, A Nandakumar, "Projections of Number of Cancer Cases in India (2010- 2020) by Cancer Groups", Asian Pacific Journal of Cancer Prevention, Vol. 11, PP. 1045-1049, 2010.
- [4] Nikita Singh, Alka Jindal, "A Segmentation Method and Comparison of Classification Methods for Thyroid Ultrasound Images", International Journal of Computer Applications (0975 – 8887) Volume 50 – No.11, PP 43-49, July 2012.
- [5] Stamos Katsigiannis, Eystratios G. et a, "A Contourlet Transform Feature Extraction Scheme for Ultrasound Thyroid Texture Classification", Engineering Intelligent Systems, Special issue: Artificial Intelligence Applications and Innovations 2010, vol. 18, no. 3/4, 2010.
- [6] Stamos Katsigiannis, Eystratios G. et al, "Contourlet Transform for Texture Representation of Ultrasound Thyroid Images", IFIP Advances in Information & communication Technology 339; 138-45 2010..
- [7] M.A. Savelonasa, D.K. Iakovidis et al, "Computational Characterization of Thyroid Tissue in the Radon Domain", Twentieth IEEE International Symposium on Computer- Based Medical Systems 0-7695-2905-4/07, 2007.
- [8] Maria E. Lyra, Katerina Skouroliakou et al, "Texture Characterization in Ultrasonograms of the Thyroid Gland", M05-301: (10:30) NSS-MIC 2009.
- [9] Dimitris K. Iakovidis , Eystratios G. Keramidas et al, "Fusion of fuzzy statistical distributions for classification of thyroid ultrasound patterns", Artificial Intelligence in Medicine 50, PP. 33–41, 2010.
- [10] Dimitris K. Iakovidis, Eystratios G. Keramidas et al, "Fuzzy Local Binary Patterns for Ultrasound Texture Characterization", Image Analysis and Recognition, Lecture Notes in Computer Science Vol. 5112, PP. 750-759, 2008,
- [11] Stavros Tsantis, Dimitris Glotsos et al, "Improving Diagnostic Accuracy In The Classification Of Thyroid Cancer By Combining Quantitative Information Extracted From Both Ultrasound And Cytological Images", 1st International Conference "From Scientific Computing to Computational Engineering" Athens, 8-10 September, 2004.
- [12] G. Castellano, L. Bonilha et al, "REVIEW Texture analysis of medical images", *Clinical Radiology* 59, PP.1061–1069, 2004.
- [13] A. Materka, M. Strzelecki, "Texture Analysis Methods – A Review", *Technical University of Lodz, Institute of Electronics, COST B11 report, Brussels, 1998.*
- [14] Shrikant D. Kale, K. M. Punwatkar, "A Different Texture Characterization Technique For Diagnosis of Thyroid Nodule Using Medical Ultrasound Images-A Survey", in *Proceeding of International Conference on Emerging Trends in Technology & its Application, Karjat, Dist. Raigad, , PP. 291-297, 6-7March 2013.*
- [15] Shrikant D. Kale, K. M. Punwatkar, "Texture Analysis of Ultrasound Medical Images for Diagnosis of Thyroid Nodule Using Support Vector Machine", *International Journal of Computer Science and Mobile Computing.*, ISSN: 2320–088X, Vol.2, Issue.10, PP. 71-77, October- 2013.
- [16] Shrikant D. Kale, K. M. Punwatkar, "Texture Analysis of Thyroid Ultrasound Images for Diagnosis of Benign and Malignant Nodule Using Scaled Conjugate Gradient Backpropagation Training Neural Network", *International Journal of Computational Engineering & Management*, ISSN: 2230-7893, Vol. 16 Issue 6, PP. 33-38, November 2013.